Environment International 185 (2024) 108487

Contents lists available at ScienceDirect

Environment International

journal homepage: www.elsevier.com/locate/envint

Full length article

Unveiling the overlooked direct emissions of particulate organic nitrates from ship

Jing Chen [a], Xiao Fu [a,*], Xinfeng Wang [b,*], Shuwei Dong [c], Tianshu Chen [d], Likun Xue [b], Yang Zhou [e], Lifang Sheng [e], Wenxing Wang [b]

[a] Institute of Environment and Ecology, Tsinghua Shenzhen International Graduate School, Tsinghua University, Shenzhen 518055, China
[b] Environment Research Institute, Shandong University, Qingdao 266237, China
[c] Guangzhou Institute of Geochemistry, Chinese Academy of Sciences, Guangzhou 510640, China
[d] Department of Civil and Environmental Engineering, Hong Kong Polytechnic University, Hong Kong 999077, China
[e] College of Oceanic and Atmospheric Sciences, Ocean University of China, Qingdao 266100, China

ARTICLE INFO

Keywords:
Particulate organic nitrates
Ship exhausts
Primary emission

ABSTRACT

Particulate organic nitrates (pONs) have drawn growing interests due to their effects on nitrogen cycling, air pollution, and regional climate. While secondary formation is typically considered as the major source of pONs, direct emissions from various sources remain poorly explored. Ship exhausts have been known as an important source of reactive nitrogen species, yet pONs emissions from ship have been rarely characterized. In this study, we conducted atmospheric measurement of pONs during a ship-based cruise measurement campaign in the East China Sea and also emission measurement of pONs from ship exhausts. During the ship-based cruise, total five typical kinds of pONs were determined and the average total concentrations of five pONs were 479 ± 193 and 250 ± 139 ng m^{-3} when sampling was influenced by ship emissions or not, respectively, indicating the notable impact of ship exhaust plumes on ambient pONs. Further, five typical pONs were successfully identified and quantified from ship exhausts, with the average total concentration of 1123 ± 406 μg m^{-3}. The much higher pONs levels in ship exhausts than in ambient particulate matters demonstrated ship emission as an important source for pONs. Additionally, their emission factors from ship exhausts were determined as at a range of 0.1–12.6 mg kWh^{-1}. The chemical transport model simulations indicate that direct pONs emissions from ship exert a significant contribution to atmospheric pONs, especially in the clean marine atmosphere. These findings provide compelling evidence for direct emission of pONs from ship and its considerable effects. We call for further studies to better characterize the direct pONs emissions from ship and other potential sources, which should be incorporated into global and regional models.

1. Introduction

Particulate organic nitrates (pONs), a class of organic compounds characterized by the presence of nitro groups (–ONO_2), are important constitutions of nitrogen-containing organic compounds (Perring et al., 2013). In its formation and transformation processes, pONs function as temporary nitrogen reservoirs, contributing to the nitrogen cycling (Lee et al., 2016; Romer Present et al., 2020). Additionally, pONs constitute a significant proportion (9–25 %) of organic aerosols (Huang et al., 2021; Kenagy et al., 2021; Lee et al., 2019; Xu et al., 2015; Yu et al., 2019), making them essential in the atmosphere. Besides, because of containing hydrophilic functional groups like hydroxyl and carboxyl groups, pONs can act as cloud condensation nuclei (CCN), affecting the global radiative balance and thereby influencing regional climate (Tegen and Schepanski, 2018). Thus, it is essential to identify the sources of atmospheric pONs in order to assess its impacts on the atmospheric environment.

Secondary formation has been reported to be the dominant sources for pONs. Volatile organic compounds (VOCs) can undergo oxidation by atmospheric oxidants (such as OH radicals, NO_3 radicals, and ozone O_3) in the presence of nitrogen oxides (NO_x) to form gaseous organic nitrates (gONs). Through partitioning mechanisms, gONs are introduced into the particulate phase, leading to the formation of pONs. Furthermore, heterogeneous reaction also represents a potential pathway for the

* Corresponding authors.
E-mail addresses: fu.xiao@sz.tsinghua.edu.cn (X. Fu), xinfengwang@sdu.edu.cn (X. Wang).

https://doi.org/10.1016/j.envint.2024.108487
Received 13 December 2023; Received in revised form 30 January 2024; Accepted 5 February 2024
Available online 14 February 2024

formation of pONs (Deng et al., 2021; Northcross and Jang, 2007; Zaveri et al., 2010). However, direct emissions, or primary sources, remains almost unexplored (Fisher et al., 2018; Perring et al., 2013), which increases the uncertainties in assessing the role of pONs in the atmospheric environment and proposes challenges for mitigating air pollution. Exhaust of diesel engine combustion have been reported to emit the precursors of pONs, such as NO_x, α-pinene, β-pinene, oleic acid (Feng, 2013; Huang et al., 2018; Rogge et al., 1993), indicating the large possibility of their direct emissions of pONs simultaneously. Ships, which are fueled by diesel usually, can be a potential primary source of pONs, which has not been investigated to date. This knowledge gap will hinder the better understanding of atmospheric chemistry and air pollution formation mechanism over coastal region and marine area, due to the key role of ship emissions in the land-sea interaction.

In this study, we conducted the ship-based measurement of ambient atmospheric pONs during a cruise campaign in the East China Sea and also direct emission measurement of pONs emissions from ship exhausts. Evidences from atmospheric observation and direct ship exhausts measurement both confirmed the presence of pONs in ship emissions. The global atmospheric chemical transport model simulation revealed that the inclusion of direct pONs emissions from ship exhausts increased atmospheric pONs over the marine regions significantly. Overall, this study provides the direct measurement evidence for direct emissions of pONs from ships, and its substantial role in contributing to atmospheric pONs, especially over marine regions, than previously assumed.

2. Experiments and methods

2.1. Atmospheric measurements during a cruise campaign

The cruise measurement campaign was conducted in the East China Sea (117-131°E, 23-33°N) on a Scientific Research Vessel called "Dong Fang Hong 2" from April 22 to May 27, 2017. Fig. S1 displays the averaged locations for each filter sample obtained during the cruise. The sampling started when the vessel was far from the shore to avoid the impact of the anthropogenic activities and vehicle emissions at the port. Furthermore, since several stops were designed along the cruise route to collect the sea-water samples, the collection of $PM_{2.5}$ samples were also temporarily paused. The sampling duration for each filter sample ranged from 6 to 23 h, depending on the level of particulate matter pollution. The sample filters were kept in a freezer at –20 °C until analysis. Details about the Scientific Research Vessel, and the real-time measurement instruments of related air pollutants and meteorological parameters can be referred to (Sun et al., 2020). In total, 33 ambient $PM_{2.5}$ samples (two of which are field blank samples) were collected with a medium-volume sampler (TH-150A, Wuhan Tianhong, China) at a flowrate of 100 L min^{-1}.

One half of sample filter (~25 cm^2) was cut from each $PM_{2.5}$ samples for a further pretreatment including ultrasonication, stationary, filtration and nitrogen evaporation to obtain the corresponding extracts for pONs determination and qualification. Detailed treatment procedures can be referred to (Chen et al., 2022). In this study, due to the complex components and limited availability of reference standards, five kinds of major pONs were analyzed using an ultra-high performance liquid chromatography (UHPLC, Thermo Scientific, USA) coupled to an ion-trap mass spectrometer (Thermo Scientific, USA) including Monoterpene hydroxyl nitrate (molecular weight (MW) = 215 g/mol, MHN215), Pinene keto nitrate (MW = 229 g/mol, PKN229), Monoterpene dicarbonyl nitrate (MW = 247 g/mol, MDCN247), Oleic acid keto nitrate (MW = 359 g/mol, OAKN359) and Oleic acid hydroxyl nitrate (MW = 361 g/mol, OAHN361). The formula, proposed structures and mass-to-charge ratio of the five kinds of quantified pONs are listed in Table S1. Details about mass spectrum condition and chromatographic condition (column, two surrogate standards, gradient elution and gradient procedure settings) can be found in (Chen et al., 2022).

2.2. Emission measurements from ship exhausts

The sample collection for ship exhausts was performed in May 2021 with the mobile measurement system mentioned in (Lu et al., 2019). It contains adjustable sampling tube, $PM_{2.5}$ sampler, gas analyzer, and exhaust flow meter, but with some modifications in the adjustable sampling part to fit the large ship exhaust outlets. $PM_{2.5}$ were collected onto a 47-mm quartz-fiber filter by Deployable Particulate Sampler System (SKC, USA) at a flow rate of 10 L min^{-1}. The sampling duration lasted for 5 min. The mixing ratios of NO, CO, CO_2 were measured using a gas analyzer (KANE AUTOplus 5–2, UK) at a time resolution of 30 s. An intelligent anemometer (DN2000, China) was used to estimate the flowrate of ship exhausts.

Total six vessels, including five wooden cargo vessels and one iron cargo vessel, were tested in operating conditions to get the emission factors (EF) of pONs. The selection of vessels covered different sizes, different fuel types, and different engine powers, as shown in Table 1. Due to the limited experimental conditions, the different operating conditions such as maneuver, berth, cruise, departure, and arrival were not strictly distinguished in this study, which may bring uncertainties to the estimation of EF of pONs.

Same pretreatment procedures described above (in Section 2.1) were used to get the organic extracts for further determinations of pONs from ship exhausts. Since more complex composition of ship exhausts, the resulting extracts were analyzed using an ultra-high performance liquid chromatography (UHPLC, Thermo Scientific, USA) equipped with a quadrupole time-of-flight mass spectrometer (TOF-MS, Bruker, Germany) and an ultra-high performance liquid chromatography (UHPLC, Thermo Scientific, USA) equipped with a triple quadrupole mass spectrometer (Thermo Scientific, USA) for identification, and the same instruments mentioned in Section 2.1 for qualification. Similar retention time and mass spectrum fragments with previous studies (Chen et al., 2022; Li et al., 2018) for the five kinds of pONs ensure the reliable determination results.

The EF of pONs were calculated according to substances (i) and ship type (j) as illustrated in the equation below (Goldsworthy and Goldsworthy, 2015):

$$EF_{i,j} = \frac{E_{i,j} \times 1000}{P_j \times LF_j \times T_{i,j}} \quad (1)$$

Here, $EF_{i,j}$ is the emission factors of substance i for ship type j in mg kWh^{-1}; $E_{i,j}$ is the emissions of substance i from ship type j in g; P_j is the power of machine engine for ship type j in kW; LF_j is the loading factors for ship type j with unitless; and $T_{i,j}$ is the sampling duration of substances i for ship type j in hour (h).

2.3. Model description

GEOS-Chem version 14.1.1 (https://geoschem.github.io) was used to investigate the potential impacts of ship pONs emissions on global

Table 1
Summary of the testing ships.

Types	Abbr.	Size (m)	Engine power (kW)	fuel type	Samples
Wooden cargo vessel −1	WV1	9 × 2	26	No.-10 Diesel	4
Wooden cargo vessel −2	WV2	11 × 2.5	29	No.-10 Diesel	3
Wooden cargo vessel −3	WV3	13 × 2.5	13	No.-10 Diesel	3
Wooden cargo vessel −4	WV4	15 × 3	110	No.0 Diesel	3
Wooden cargo vessel −5	WV5	24 × 5	206	No.0 Diesel	2
Iron cargo vessel	IV	19.8 × 5	219	No.0 Diesel	3

pONs concentration. MHN215 was chosen as a representative pONs species because its chemical mechanisms have been updated in GEOS-Chem model, including monoterpene oxidation chemistry (the OH oxidation and NO_3 oxidation mechanisms), gas-particle partitioning, hydrolysis and photolysis loss mechanisms. The model was driven by assimilated meteorological input from the Goddard Earth Observing System (GEOS) of NASA Global Modeling and Assimilation Office (GMAO) (Bey et al., 2001). In this study, MERRA-2 was selected for the meteorology data source. The model was run with a resolution of 4° latitude × 5° longitude and 72 vertical layers under the full chemistry mode (NO_x-O_x-HC-Aerosol-Br-Cl-I chemistry). The year 2017 was chosen as the simulation year since the cruise measurement campaign was conducted during that year and a two-year spin-up simulation was performed to provide initial conditions for the target simulation. Besides, global emission inventories CEDSv2 (for anthropogenic and ship CO, NO_x, NH_3, SO_2, VOCs, BC, OC, CO_2), AEIC (for aircraft CO, NO_x, SO_2, VOCs, BC, OC), GFED4 (for biomass burning emissions), MEGAN (for biogenic VOCs emissions) and GEIA (for natural sources NH_3) were used for simulation input (Bouwman et al., 1997; Giglio et al., 2013; Guenther et al., 2012; Hoesly et al., 2019.; Lin et al., 2021; Stettler et al., 2011). The global ship emissions of MHN215 was estimated by the relative emission factors (*rEF*) as defined in Eq. (2) and the ship NO emissions from CEDSv2.

$$rEF = \frac{EF_{MHN215}}{EF_{NO}} \tag{2}$$

Here, EF_{MHN215} and EF_{NO} are the emission factors of MHN215 and NO as mass per kWh of engine (mg kWh^{-1}), respectively, which are derived from our measurements of ship exhaust emissions. A *rEF* of 5.17 × 10^{-4} was adopted in this study based on the calculated average results of sampling vessels.

The model was run with and without ship emissions inventory of MHN215 (denoted as 'WithShipONs' and 'Base', respectively), and differences between these two simulations are regarded as the effects of the ship-emitted MHN215. Note that due to the incomplete emission inventory and reaction mechanisms for pONs and their precursors, the modelling simulation by GEOS-Chem in this study is subjected to some uncertainty. Previous field observations on MHN215 observations are very limited, especially over ocean region. Comparing with the available observation data in inland sites (Chen et al., 2022; Li et al., 2018; Zhang et al., 2021; Zhang et al., 2020) where secondary formation is dominant, the simulated MHN215 concentrations are underestimated by approximately 80 %, indicating incomplete secondary formation mechanisms and ignoration of potential additional sources in the GEOS-Chem model. Similarly, an observation-based chemical box model for MHN215 production rate simulation in a previous study also revealed the underestimation (approximately 2 to 7-fold lower) because of the absence mechanism of ozone oxidation and heterogeneous reactions (Zhang et al., 2020). Thus, the 'Base' scenario simulation result was scaled up by a factor of 5 (denoted as Base*) to better represent the base MHN215 from secondary formation. Absolute difference driven by ship emissions of MHN215 was calculated using the unscaled 'Base' and 'WithShipONs' scenarios. And relative difference referred to the change ratio of absolute difference relative to the 'Base*' scenario instead of 'Base' scenario.

3. Results and conclusions

3.1. Evidence from atmospheric observations

Fig. 1 shows the time series of the concentrations of five kinds of pONs, mixing ratios of gaseous pollutants and meteorological conditions during the ship-based cruise measurement campaign in the East China sea. As shown, the high concentrations of pONs and the spikes in the mixing ratios of NO, NO_2 were frequently accompanied during entire

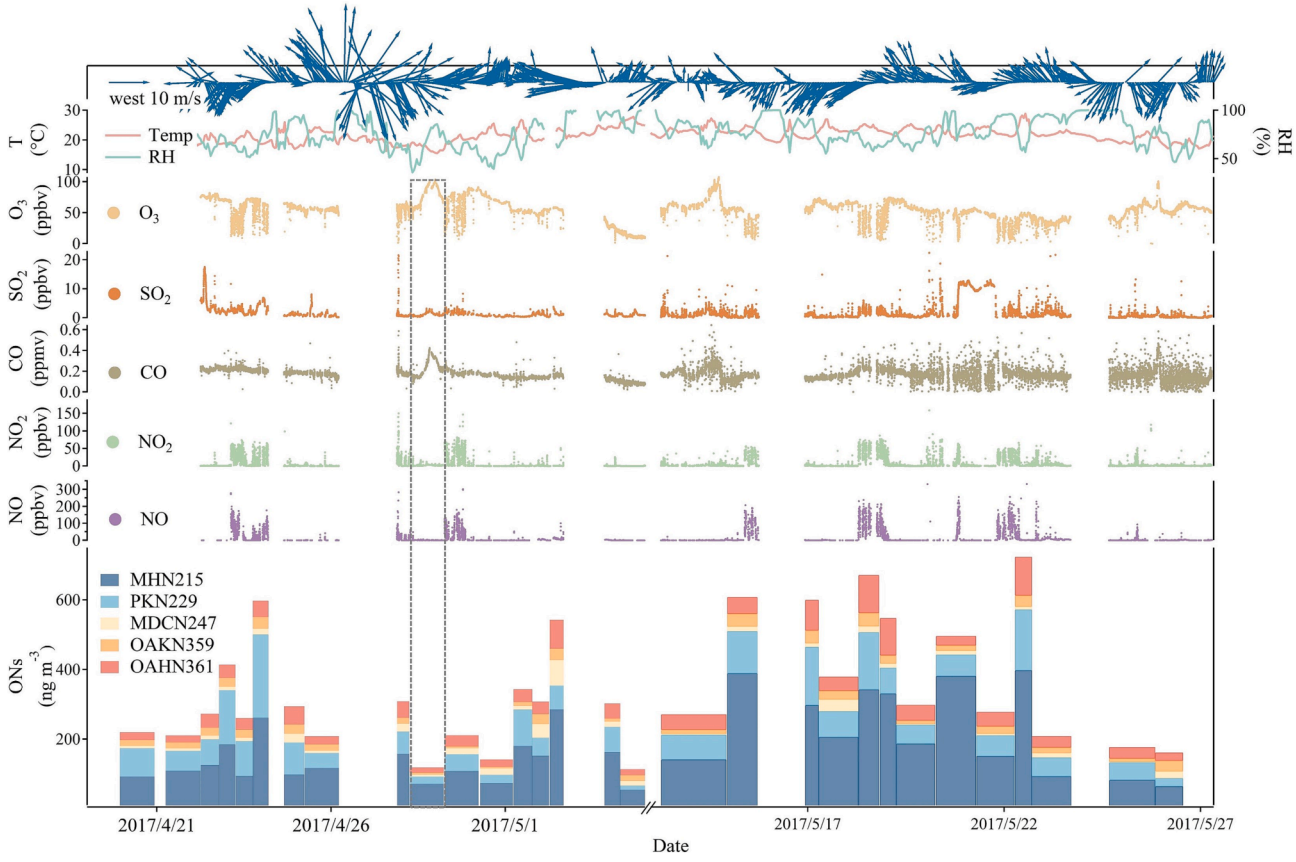

Fig. 1. Time series of the concentrations of five kinds of pONs, mixing ratios of gaseous pollutants, and meteorological conditions.

campaign (e.g., On 23 April, 27 April, 14 May, 18 May and 22 May). Regarding the typical high-value cases during the sampling periods, the maximum and second highest concentration of the total concentrations of five pONs (ΣONs) were observed on May 22 and May 18, with values of 724 and 672 ng m^{-3}, respectively. In these two cases, the mixing ratio of NO both exceeded 200 ppbv with similar southeast wind. Since NO is a typical primary pollutant of ship exhausts, therefore, it is possible that pollutants from ship exhaust plumes affect the concentration of pONs by transport when the wind came from the stern. Further grouping analysis was conducted to confirm this impact. NO was used as an indicator of ship emissions, and the samples were categorized into two groups: those influenced by ship exhaust (named ICs, the average mixing ratio of NO > 20 ppbv with the presence of concentration spikes) and those unaffected by ship exhaust (named UCs, the average mixing ratio of NO < 5 ppbv with a stable NO concentration). As a result, a total of 9 cases were identified as being influenced by ship emissions, while 13 cases were characterized as having no discernible influence from ship exhaust emissions. The average concentration of ΣONs, MHN215, PKN229, OAKN359 and OAHN361 in ICs were found to be 1.9, 2.0, 2.2, 1.4, 1.9 times higher than those in UCs. This values further emphasizing the notable impact of ship exhaust plumes on ambient pONs.

In addition, the average concentrations of MHN215, PKN229, MDCN247, OAKN359, and OAHN361 during this cruise measurement campaign were 176.0 ± 106.5, 80.0 ± 52.6, 15.1 ± 13.8, 20.7 ± 9.9, and 44.3 ± 27.0 ng m^{-3} (mean ± standard deviations), respectively, which are comparable with the pONs level observed in urban and suburban areas (Table S2) (Chen et al., 2022; Li et al., 2018; Zhang et al., 2021; Zhang et al., 2020). In the marine atmosphere, secondary formation of pONs is hindered due to limited pONs precursors, implying the potential significant contributions of ship emissions to the observed high pONs concentrations.

To examine the potential influence of long-range transport of polluted air masses to the concentration of pONs (Sadanaga et al., 2019; Salvador et al., 2020), the concentration and variation of CO were inspected in detail, with consideration of its long atmospheric lifetime and relatively low reactivity. In this ship cruise campaign, the average mixing ratio of CO was 167 ± 63 ppbv, comparable with the non-polluted marine air CO concentration over the Pacific (50–200 ppbv of background marine CO concentration while greater than 400 ppbv when influenced by pollution plumes exported from the continent) (Clark et al., 2015), suggesting a minor influence from the long-distance transport of polluted air masses. Slightly high level of CO was observed on April 28, when it exceeded 300 ppbv continuously for 6 h period (as shown in Fig. 1, marked by the gray dashed lines). At the same time, the mixing ratios of NO_x and SO_2 were relatively low which excluded the influence of ship emissions. However, during this period, the levels of pONs remained relatively low, indicating that long-distance transport was not the dominant factor controlling the abundances of pONs in this campaign.

3.2. Evidence from direct emission measurements

To further evaluate whether ship exhausts can release organic nitrates, direct emission measurements of ship exhausts were conducted. In total, five typical kinds of pONs including MHN215, PKN229, MDCN247, OAKN359 and OAHN361 were successfully detected. Table 2 shows the concentrations of five kinds of pONs, the total concentration of five kinds of pONs (ΣONs), $PM_{2.5}$, ΣONs/$PM_{2.5}$, CO_2, CO, and NO detected from the ship exhaust determinations. The average ΣONs varied from 802 to 1346 μg m^{-3} and the concentration of individual pONs ranged from 8.8 to 569.1 μg m^{-3}. The highest concentration of ΣONs reached up to 1821 μg m^{-3}, indicating considerable ship exhaust emissions compared with terrestrial secondary formation (0.01–2.94 μg m^{-3}) of pONs (Chen et al., 2022; Li et al., 2018; Li et al., 2021; Zhang et al., 2021; Zhang et al., 2020). The proportion of ΣONs to $PM_{2.5}$ (ΣONs/$PM_{2.5}$) was at a range of 2.1–13.0 % (with average value of 4.9 % in six experiment vessels samples) which was higher than the observation results in the Mountain sites (1 %) (Chen et al., 2022) as well as urban and suburban sites (1.6–3.9 ‰) (Li et al., 2018; Zhang et al., 2021).

Table 2
Concentrations of five kinds of pONs, $PM_{2.5}$, CO_2, CO and NO from ship emissions (in μg m^{-3} for pONs and ΣONs, in mg m^{-3} for $PM_{2.5}$, in % for ΣONs/ $PM_{2.5}$, CO_2 and CO, and in ppmv for NO).

Types	WV1	WV2	WV3	WV4	WV5	IV
MHN215	288.0 ± 123.4	217.1 ± 43.8	238.4 ± 137.1	294.4 ± 196.5	212.3 ± 0.5	218.7 ± 65.7
PKN229	542.9 ± 290.6	492.7 ± 64.5	442.8 ± 272.0	569.1 ± 461.0	363.7 ± 54.2	319.3 ± 164.3
MDCN247	295.5 ± 182.7	291.7 ± 72.7	165.3 ± 100.1	71.9 ± 16.7	537.6 ± 226.2	54.3 ± 14.0
OAKN359	82.4 ± 16.8	286.3 ± 83.2	133.5 ± 15.3	82.0 ± 24.2	208.7 ± 17.5	201.4 ± 54.6
OAHN361	78.1 ± 19.8	11.1 ± 7.8	19.2 ± 1.9	9.3 ± 3.9	23.5 ± 11.3	8.8 ± 3.7
ΣONs	1287 ± 393	1299 ± 167	999 ± 516	1027 ± 699	1346 ± 201	802 ± 167
$PM_{2.5}$	63.6 ± 15.9	19.8 ± 2.9	44.1 ± 6.3	13.5 ± 0.2	58.4 ± 8.0	9.8 ± 0.2
ΣONs/ $PM_{2.5}$	2.1 ± 0.8	6.8 ± 1.9	2.3 ± 1.1	7.5 ± 5.0	2.4 ± 0.7	8.2 ± 1.8
CO_2	1.2 ± 0.05	1.8 ± 0.5	3.1 ± 0.2	3.4 ± 0.6	6.7 ± 0.5	–
CO	0.02 ± 0.005	0.04 ± 0.012	0.02 ± 0.004	0.02 ± 0.001	0.02 ± 0.011	–
NO	316 ± 88	199 ± 21	561 ± 87	480 ± 31	1063 ± 39	–

Based on Eq. (1), the emission factors of the five kinds of pONs emitted from ship exhausts were calculated, as listed in Table 3. Since there were numerous researches of ordinary pollutants other than pONs, emission factors of $PM_{2.5}$, NO, CO and CO_2 were chosen to compare for the reasonableness assessment. As shown in Table S3, the emission factors of $PM_{2.5}$, NO, CO and CO_2 in this study are comparable with other studies, indicating the measurement reliability of pONs' emission factors obtained in this study (Chu-Van et al., 2018; Huang et al., 2018; Khan et al., 2012; Sippula et al., 2014; Yang et al., 2022; Zhang et al., 2016).

The emission factors of pONs exhibited large discrepancies for different fuel types and vessel types, with the total factors at a range of 8.0–31.0 mg kWh^{-1} and individual factors in the level of 0.1–12.6 mg kWh^{-1}. Among the five kinds of pONs, PKN229 has the highest mean emission factor (ranged from 2.1 to 12.6 mg kWh^{-1}), while OAHN361 has the lowest. Overall, the emission factors for pONs derived from monoterpenes (MHN215, PKN229 and MDCN247) exceed those originating from oleic acid (OAKN359 and OAHN361).

Various aspects affect emission factors of pONs. Ship exhausts treatment primarily hinges on factors such as vessel size, fuel type, emission regulations, and technological availability. Notably, small vessels exhibit higher emission factors of pONs. Specifically, the emission factors of MHN215, PKN229, MDCN247, OAKN359 and OAHN361 of the largest vessel, WV5, were 1.2, 2.1, 3.3, 1.2, 0.1 mg kWh^{-1}, respectively, while were much higher for WV1, the smallest vessel. Small vessels are typically constrained by limitations in space and resources, which often preclude the installation of large-scale exhaust treatment systems, commonly rely on simpler emission control technologies. In contrast, large vessels typically employ advanced exhaust treatment technologies, resulting in lower pONs emissions. Besides, different fuel types also influence the emission factors of pONs, with No.-10 diesel (for WV1, WV2 and WV3) being higher than No.0 diesel fuel (for WV4, WV5 and IV). Generally, No.-10 diesel tends to exhibit relatively higher emissions of nitrogen oxides (NO_x) than No.0 diesel because of the less complete combustion associated with higher sulfur content. Therefore, the pONs emission factors are higher for vessels

Table 3
Emissions factors of five kinds of pONs from ship exhausts. (unit: mg kWh^{-1}).

Types	MHN215	PKN229	MDCN247	OAKN359	OAHN361	ΣONs
WV1	6.8	12.6	7.6	2.1	1.9	31.0
WV2	3.6	8.2	4.9	4.7	0.2	21.6
WV3	2.3	4.3	1.6	1.3	0.2	9.8
WV4	2.6	4.9	0.6	0.7	0.1	9.0
WV5	1.2	2.1	3.3	1.2	0.1	8.0
IV	2.4	3.5	0.6	2.3	0.1	8.9
Mean	3.2	5.9	3.1	2.1	0.4	14.7

fueled by No.-10 diesel, emphasizing the pivotal role of NO_x as a significant intermediate in the formation of pONs.

3.3. Impacts of direct pONs emissions from ships on atmospheric pONs

The GEOS-Chem model was used to investigate the impacts of ship pONs emissions on global pONs concentration, with MHN215 as a representative pONs species due to its secondary formation mechanism involved in the GEOS-Chem model. Fig. 2 shows the spatial distribution of simulated pONs concentrations without ship pONs emissions, and the absolute and relative difference after incorporating ship emissions inventory of MHN215. Without considering ship emissions of MHN215, the simulated global distributions of MHN215 in marine atmospheres were very low, averaging 1.4 ng m^{-3}, with 50 % of values below 3×10^{-4} ng m^{-3} and high values often appeared in coastal areas. These simulated low concentrations can be potentially attributed to no other direct MHN215 emission sources and limited secondary formation of MHN215 due to the scarcity of precursors in marine areas. In addition, underestimation of the secondary formation of MHN215 due to incomplete emission inventory and formation mechanisms of MHN215 in the GEOS-Chem model also could be another possible reason. The inclusion of ship pONs emissions increased atmospheric pONs concentration over the ocean significantly, with a mean factor of 11 times. The large increases occured in the regions with dense shipping activities, such as East Asia - Pacific from approximately 140°E to 140°W longitude and 20°N to 55°N latitude, Atlantic from roughly 20°W to 60°W longitude and 20°N to 60°N latitude, the India ocean covering about 60°E to 80°E longitude and 5°S to 25°S latitude. Notably, in the Antarctic region with limited shipping activities, MHN215 exhibited remarkable increases driven by the ship pONs emissions. The reason can be attributed to the influence of atmospheric transport. Research has found that ship emissions (mainly from tourists visiting Antarctica and fishing vessels) from south of 60°S, contributed to half of the total black carbon (typical primary pollutant) within south of 70°S through transport (Stohl and Sodemann, 2010). Thus, as the lifetime of organic nitrate can be several days to several month (Clemitshaw et al., 1997), longer in cold season (Sadanaga et al., 2019), it is likely that ship-emitted long-lived MHN215 has been transported to these pristine regions, resulting in significant relative variations owing to relatively low background concentrations.

3.4. Discussion

Organic nitrates are important nitrogen-containing organic compounds due to their influence on atmospheric chemistry and air quality. In this study, direct emissions of pONs from ships were confirmed through atmospheric measurements and ship exhausts determinations. Global chemical transport model simulation results highlight the considerable contributions of ship pONs emissions on the concentrations of pONs over marine regions. This is a pilot study to investigate the characteristics and impacts of direct pONs emissions from ships, and large uncertainties still exist for our estimation. For example, the measurements of ship exhausts were conducted mainly for small and middle vessels, and more measurements for large vessels are needed in the future. Additionally, due to the complex components and limited availability of reference standards of organic nitrates, only five kinds of pONs were identified in this study, which may underestimate the total pONs emissions from ships and their impacts. Furthermore, the model simulations only focus on one representative species, due to limited chemical mechanism of pONs formation and transformation involved in the global model. More pONs species and more complete pONs chemical mechanism should be incorporated into the model in the future.

In despite of the uncertainties, this study provides compelling evidence for direct emission of pONs from ship and its considerable effects for the first time, which have been overlooked previously. We recommend that greater attention should be paid to direct pONs emissions from ships and also other potential primary sources to achieve better understanding of the role of pONs in the atmospheric environment.

CRediT authorship contribution statement

Jing Chen: Writing – review & editing, Writing – original draft, Methodology, Investigation, Formal analysis. **Xiao Fu:** . **Xinfeng Wang:**

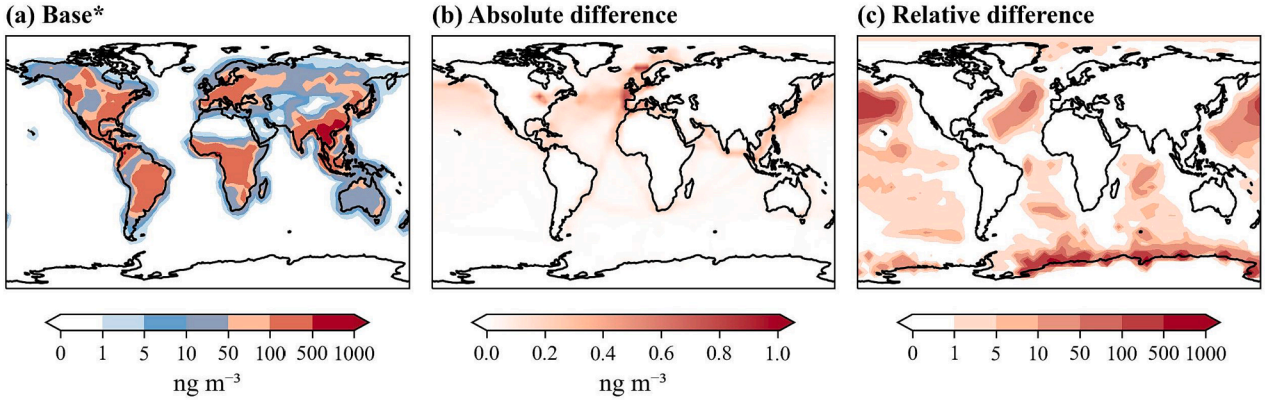

Fig. 2. (a) The global distributions of simulated MHN215 in 2017 in the Base* scenario. (b, c) Absolute difference and relative difference of global distributions of simulated MHN215 with and without ship emissions of MHN215.

Writing – review & editing, Supervision, Methodology, Funding acquisition, Conceptualization. **Shuwei Dong:** Investigation. **Tianshu Chen:** Investigation. **Likun Xue:** Resources. **Yang Zhou:** Resources. **Lifang Sheng:** Resources. **Wenxing Wang:** Resources.

Declaration of competing interest

The authors declare that they have no known competing financial interests or personal relationships that could have appeared to influence the work reported in this paper.

Data availability

Data will be made available on request.

Acknowledgements

This work was supported by National Natural Science Foundation of China (22206106, 42377094), Municipal Science and Technology Innovation Commission of Shenzhen (JCYJ20220530143007016), Natural Science Foundation of Guangdong Province (2022A1515010705), and Scientific Research Start-up Funds from Tsinghua Shenzhen International Graduate School (QD2021015C).

Appendix A. Supplementary material

Supplementary data to this article can be found online at https://doi.org/10.1016/j.envint.2024.108487.

References

Bey, I., Jacob, D.J., Yantosca, R.M., Logan, J.A., Field, B.D., Fiore, A.M., Li, Q.B., Liu, H. G.Y., Mickley, L.J., Schultz, M.G., 2001. Global modeling of tropospheric chemistry with assimilated meteorology: Model description and evaluation. J. Geophys. Res.-Atmos. 106, 23073–23095.

Bouwman, A.F., Lee, D.S., Asman, W.A.H., Dentener, F.J., Van Der Hoek, K.W., Olivier, J. G.J., 1997. A global high-resolution emission inventory for ammonia. Glob. Biogeochem. Cycle 11, 561–587.

Chen, J., Wang, X., Zhang, J., Li, M., Li, H., Liu, Z., Bi, Y., Wu, D., Yin, X., Gu, R., Jiang, Y., Shan, Y., Zhao, Y., Xue, L., Wang, W., 2022. Particulate organic nitrates at Mount Tai in winter and spring: Variation characteristics and effects of mountain-valley breezes and elevated emission sources. Environ. Res. 212, 113182.

Chu-Van, T., Ristovski, Z., Pourkhesalian, A.M., Rainey, T., Garaniya, V., Abbassi, R., Jahangiri, S., Enshaei, H., Kam, U.S., Kimball, R., Yang, L.P., Zare, A., Bartlett, H., Brown, R.J., 2018. On-board measurements of particle and gaseous emissions from a large cargo vessel at different operating conditions. Environ. Pollut. 237, 832–841.

Clark, H.; Sauvage, B.; Thouret, V.; Nédélec, P.; Blot, R.; Wang, K.Y.; Smit, H.; Neis, P.; Petzold, A.; Athier, G.; Boulanger, D.; Cousin, J.M.; Beswick, K.; Gallagher, M.; Baumgardner, D.; Kaiser, J.; Flaud, J.M.; Wahner, A.; Volz-Thomas, A.; Cammas, J. P., 2015. The first regular measurements of ozone, carbon monoxide and water vapour in the Pacific UTLS by IAGOS. Tellus. Ser. B-Chem. Phys. Meteorol. 67.

Clemitshaw, K.C., Williams, J., Rattigan, O.V., Shallcross, D.E., Law, K.S., Cox, R.A., 1997. Gas-phase ultraviolet absorption cross-sections and atmospheric lifetimes of several C2–C5 alkyl nitrates. J. Photochem. Photobiol. A-Chem. 102, 117–126.

Deng, H., Liu, J., Wang, Y., Song, W., Wang, X., Li, X., Vione, D., Gligorovski, S., 2021. Effect of inorganic salts on N-containing organic compounds formed by heterogeneous reaction of NO_2 with oleic acid. Environ. Sci. Tech. 55, 7831–7840.

Feng, X.Q., 2013. Study on the Emission Characteristics of VOCs and $PM_{2.5}$ from Motor Vehicles in the Pearl River Delta. South China University of Technology.

Fisher, J.A., Atlas, E.L., Barletta, B., Meinardi, S., Blake, D.R., Thompson, C.R., Ryerson, T.B., Peischl, J., Tzompa-Sosa, Z.A., Murray, L.T., 2018. Methyl, ethyl, and propyl nitrates: global distribution and impacts on reactive nitrogen in remote marine environments. J. Geophys. Res.-Atmos. 123, 12429–12451.

Giglio, L., Randerson, J.T., van der Werf, G.R., 2013. Analysis of daily, monthly, and annual burned area using the fourth-generation global fire emissions database (GFED4). J. Geophys. Res.-Biogeosci. 118, 317–328.

Goldsworthy, L., Goldsworthy, B., 2015. Modelling of ship engine exhaust emissions in ports and extensive coastal waters based on terrestrial AIS data – an Australian case study. Environ Modell Softw 63, 45–60.

Guenther, A.B., Jiang, X., Heald, C.L., Sakulyanontvittaya, T., Duhl, T., Emmons, L.K., Wang, X., 2012. The Model of Emissions of Gases and Aerosols from Nature version 2.1 (MEGAN2.1): an extended and updated framework for modeling biogenic emissions. Geosci. Model Dev. 5, 1471–1492.

Hoesly, R., O'Rourke, Patrick, Braun, Caleb, Feng, Leyang, Smith, Steven J., Pitkanen, Tyler, Seibert, Jonathan J., Vu, Linh, Presley, Muwan, Bolt, Ryan, Goldstein, Ben, Kholod, Nazar, 2019. Community Emissions Data System (Dec-23-2019). Zenodo. https://doi.org/10.5281/zenodo.3592073. 2019.

Huang, C., Hu, Q.Y., Wang, H.Y., Qiao, L.P., Jing, S.A., Wang, H.L., Zhou, M., Zhu, S.H., Ma, Y.G., Lou, S.R., Li, L., Tao, S.K., Li, Y.J., Lou, D.M., 2018. Emission factors of particulate and gaseous compounds from a large cargo vessel operated under real-world conditions. Environ. Pollut. 242, 667–674.

Huang, W., Yang, Y., Wang, Y., Gao, W., Li, H., Zhang, Y., Li, J., Zhao, S., Yan, Y., Ji, D., Tang, G., Liu, Z., Wang, L., Zhang, R., Wang, Y., 2021. Exploring the inorganic and organic nitrate aerosol formation regimes at a suburban site on the North China Plain. Sci. Total Environ. 768, 144538.

Kenagy, H.S., Romer Present, P.S., Wooldridge, P.J., Nault, B.A., Campuzano-Jost, P., Day, D.A., Jimenez, J.L., Zare, A., Pye, H.O.T., Yu, J., Song, C.H., Blake, D.R., Woo, J. H., Kim, Y., Cohen, R.C., 2021. Contribution of organic nitrates to organic aerosol over South Korea during KORUS-AQ. Environ. Sci. Tech.

Khan, M.Y., Agrawal, H., Ranganathan, S., Welch, W.A., Miller, J.W., Cocker 3rd., D.R., 2012. Greenhouse gas and criteria emission benefits through reduction of vessel speed at sea. Environ. Sci. Tech. 46, 12600–12607.

Lee, A.K.Y., Adam, M.G., Liggio, J., Li, S.M., Li, K., Willis, M.D., Abbatt, J.P.D., Tokarek, T.W., Odame-Ankrah, C.A., Osthoff, H.D., Strawbridge, K., Brook, J.R., 2019. A large contribution of anthropogenic organo-nitrates to secondary organic aerosol in the Alberta oil sands. Atmos. Chem. Phys. 19, 12209–12219.

Lee, B.H., Mohr, C., Lopez-Hilfiker, F.D., Lutz, A., Hallquist, M., Lee, L., Romer, P., Cohen, R.C., Iyer, S., Kurten, T., Hu, W., Day, D.A., Campuzano-Jost, P., Jimenez, J. L., Xu, L., Ng, N.L., Guo, H., Weber, R.J., Wild, R.J., Brown, S.S., Koss, A., de Gouw, J., Olson, K., Goldstein, A.H., Seco, R., Kim, S., McAvey, K., Shepson, P.B., Starn, T., Baumann, K., Edgerton, E.S., Liu, J., Shilling, J.E., Miller, D.O., Brune, W., Schobesberger, S., D'Ambro, E.L., Thornton, J.A., 2016. Highly functionalized organic nitrates in the southeast United States: contribution to secondary organic aerosol and reactive nitrogen budgets. PNAS 113, 1516–1521.

Li, W., Huang, S., Yuan, B., Guo, S., Shao, M., 2021. Mechanism, measurement techniques and their application for particulate organonitrates. China Environ. Sci. 41, 3017–3028.

Li, R., Wang, X.F., Gu, R.R., Lu, C.Y., Zhu, F.P., Xue, L.K., Xie, H.J., Du, L., Chen, J.M., Wang, W.X., 2018. Identification and semi-quantification of biogenic organic nitrates in ambient particulate matters by UHPLC/ESI-MS. Atmos. Environ. 176, 140–147.

Lin, H., Jacob, D.J., Lundgren, E.W., Sulprizio, M.P., Keller, C.A., Fritz, T.M., Eastham, S. D., Emmons, L.K., Campbell, P.C., Baker, B., Saylor, R.D., Montuoro, R., 2021. Harmonized Emissions Component (HEMCO) 3.0 as a versatile emissions component for atmospheric models: application in the GEOS-Chem, NASA GEOS, WRF-GC, CESM2, NOAA GEFS-Aerosol, and NOAA UFS models. Geosci. Model Dev. 14, 5487–5506.

Lu, C.Y., Wang, X.F., Dong, S.W., Zhang, J., Li, J., Zhao, Y.A., Liang, Y.H., Xue, L.K., Xie, H.J., Zhang, Q.Z., Wang, W.X., 2019. Emissions of fine particulate nitrated phenols from various on-road vehicles in China. Environ. Res. 179.

Northcross, A.L., Jang, M., 2007. Heterogeneous SOA yield from ozonolysis of monoterpenes in the presence of inorganic acid. Atmos. Environ. 41, 1483–1493.

Perring, A.E., Pusede, S.E., Cohen, R.C., 2013. An observational perspective on the atmospheric impacts of alkyl and multifunctional nitrates on ozone and secondary organic aerosol. Chem. Rev. 113, 5848–5870.

Rogge, W.F., Hildemann, L.M., Mazurek, M.A., Cass, G.R., Simoneit, B.R.T., 1993. Sources of fine organic aerosol.2. Noncatalyst and catalyst-equipped automobiles and heavy-duty diesel trucks. Environ. Sci. Tech. 27, 636–651.

Romer Present, P.S., Zare, A., Cohen, R.C., 2020. The changing role of organic nitrates in the removal and transport of NO_x. Atmos. Chem. Phys. 20, 267–279.

Sadanaga, Y., Ishiyama, A., Takaji, R., Matsuki, A., Kato, S., Sato, K., Osada, K., Bandow, H., 2019. Behavior of total peroxy and total organic nitrate concentrations at Suzu on the Noto Peninsula, Japan: long-range transport and local photochemical production. Atmos. Environ. 196, 20–26.

Salvador, C.M.; Chou, C.C.K.; Cheung, H.C.; Ho, T.T.; Tsai, C.Y.; Tsao, T.M.; Tsai, M.J.; Su, T.C., 2020. Measurements of submicron organonitrate particles: Implications for the impacts of NOx pollution in a subtropical forest. Atmos. Res. 245.

Sippula, O., Stengel, B., Sklorz, M., Streibel, T., Rabe, R., Orasche, J., Lintelmann, J., Michalke, B., Abbaszade, G., Radischat, C., Groger, T., Schnelle-Kreis, J., Harndorf, H., Zimmermann, R., 2014. Particle emissions from a marine engine: chemical composition and aromatic emission profiles under various operating conditions. Environ. Sci. Tech. 48, 11721–11729.

Stettler, M.E.J., Eastham, S., Barrett, S.R.H., 2011. Air quality and public health impacts of UK airports. Part i: Emissions. Atmos. Environ. 45, 5415–5424.

Stohl, A., Sodemann, H., 2010. Characteristics of atmospheric transport into the Antarctic troposphere. J. Geophys. Res. 115.

Sun, L., Chen, T., Jiang, Y., Zhou, Y., Sheng, L., Lin, J., Li, J., Dong, C., Wang, C., Wang, X., Zhang, Q., Wang, W., Xue, L., 2020. Ship emission of nitrous acid (HONO) and its impacts on the marine atmospheric oxidation chemistry. Sci. Total Environ. 735, 139355.

Tegen, I., Schepanski, K., 2018. Climate feedback on aerosol emission and atmospheric concentrations. Curr. Clim. Chang. Rep. 4, 1–10.

Xu, L., Suresh, S., Guo, H., Weber, R.J., Ng, N.L., 2015. Aerosol characterization over the southeastern United States using high-resolution aerosol mass spectrometry: spatial and seasonal variation of aerosol composition and sources with a focus on organic nitrates. Atmos. Chem. Phys. 15, 7307–7336.

Yang, L., Zhang, Q.J., Zhang, Y.J., Lv, Z.Y., Wu, L., Mao, H.J., 2022. Real-world emission characteristics of an ocean-going vessel through long sailing measurement. Sci. Total Environ. 810.

Yu, K.Y., Zhu, Q., Du, K., Huang, X.F., 2019. Characterization of nighttime formation of particulate organic nitrates based on high-resolution aerosol mass spectrometry in an urban atmosphere in China. Atmos. Chem. Phys. 19, 5235–5249.

Zaveri, R.A.; Berkowitz, C.M.; Brechtel, F.J.; Gilles, M.K.; Hubbe, J.M.; Jayne, J.T.; Kleinman, L.I.; Laskin, A.; Madronich, S.; Onasch, T.B.; Pekour, M.S.; Springston, S. R.; Thornton, J.A.; Tivanski, A.V.; Worsnop, D.R., 2010. Nighttime chemical evolution of aerosol and trace gases in a power plant plume: Implications for secondary organic nitrate and organosulfate aerosol formation, NO_3 radical chemistry, and N_2O_5 heterogeneous hydrolysis. J. Geophys. Res.-Atmos. 115.

Zhang, F., Chen, Y.J., Tian, C.G., Lou, D.M., Li, J., Zhang, G., Matthias, V., 2016. Emission factors for gaseous and particulate pollutants from offshore diesel engine vessels in China. Atmos. Chem. Phys. 16, 6319–6334.

Zhang, J., Wang, X.F., Zhang, Y.N., Gu, R.R., Xia, M., Li, H., Dong, S.W., Xue, L.K., Wu, Z. H., Zhang, Y.J., Gao, J., Wang, T., Wang, W.X., 2020. Pollution characteristics and formation of particulate organic nitrates in winter in Beijing City. Geochimica 49, 252–261.

Zhang, J., Wang, X.F., Li, R., Dong, S.W., Chen, J., Zhang, Y.N., Zheng, P.G., Li, M., Chen, T.S., Liu, Y.H., Xue, L.K., Zhou, X.H., Du, L., Zhang, Q.Z., Wang, W.X., 2021. Significant impacts of anthropogenic activities on monoterpene and oleic acid-derived particulate organic nitrates in the North China Plain. Atmos. Res. 256.